J. Plasma Fusion Res. SERIES, Vol. 8 (2009)

Alternative Fusion Reactors as Future Commercial Power Plants

Sergei V. RYZHKOV

Bauman Moscow State Technical University

(Received: 29 August 2008 / Accepted: 1 April 2009)

Alternative reactor based on a field-reversed configuration (FRC) has advantages of the cylindrical geometry, the open field line geometry (direct energy conversion (DEC) of the charged-particle flow), and high β (plasma pressure/magnetic-field pressure). This paper aims to evaluate the attractiveness of a low radioactive FRC fusion core. Analysis of a conceptual deuterium - helium-3 (D-^{3}He) fusion power reactor is presented and reference point is defined. Principal parameters of the D-^{3}He plasma reference case (RC) and comparison with conceptual D-^{3}He tokamak and FRC power plants are shown.

Keywords: advanced fuel, alternative concept, aneutronic reactions, bremsstrahlung, compact toroid, field reversed configuration, low radioactive reactor, magnetic confinement.

1. Introduction

The FRC [1,2] is a confinement device (FRC plasma is a toroid with the exclusively poloidal magnetic field) combining of properties and prospects of the open and closed magnetic system and leading to very large reactor advantages (see Fig. 1). Actually, FRC experiment was started in Russia (TRINITI) and USA (LANL) in 1970s. Review papers have been published in the 1980s [3,4]. Stages of FRC formation include: 1) preionization; 2) field reversal; 3) radial compression and field line connection; 4) axial contraction; and 5) equilibrium.

Since FRCs have traditionally been formed in theta-pinches, they are generally shown horizontal in contrast with the depiction of other toroidal plasmas. The FRC acts as an excluded flux object or an infinitely conducting object bounded by it separatrix.

The FRC plasma can even be formed by merging spheromaks of nearly opposite helicities, indicating a high state of self-organization.

The rotating magnetic field (RMF) power current-drive is the power required to replaced the magnetic energy dissipation caused by resistive friction. In contrast to theta-pinch RMF provides confinement.

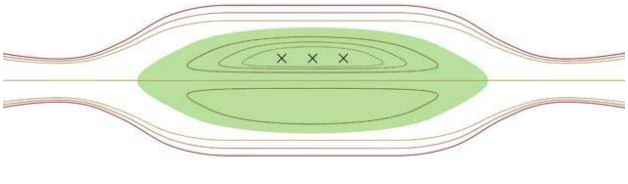

Fig.1 Magnetic flux in the elongated FRC. Closed field lines are inside the separatrix (green), open field lines are purely poloidal field (violet). The direction of azimuthal current is shown by crosses.

author's e-mail: ryzhkov@power.bmstu.ru

The main advantage of RMF is that as plasma shaping or ion beams RMF would be needed for stability.

Various plasma parameters are given in [5] for RMF formed plasmas and theta-pinch formed plasmas. Appropriate hot, steady-state FRCs can now be formed using RMF and scaling laws developed for achievable RMF sustained FRC flux levels [6].

Current drive rotating magnetic fields has been extensively explored in a series of spherical rotamak (oblate FRC) experiments at Flinders University in Australia [7]. The most extensive development of RMF current drive in more standard prolate FRCs, inside a flux conserver, has been carried out in the TCSU experiment at the University of Washington [8].

The possibility of using the whole energy of the fusion reaction directly thru the DEC system is very attractive. A FRC burning low radioactive fuel has: less complexity - simple cylindrical geometry, low activation - relative easy maintenance, and effective ash removal - natural divertor. This paper aims to evaluate the attractiveness of a steady state D-^{3}He FRC fusion power plant as future commercial reactor based on RMF current drive for startup and sustainment.

The aneutronic reactions used in the analysis of advanced fuels and alternative schemes are very sensitive to nuclear reaction cross sections and fusion reaction rate. Improved formulas for fusion cross-sections and thermal reactivities may be found in [9-12].

From the point of view of the radioactivity effects the fusion reactions can be separated in two categories, according to the case where they include radioactive elements in the reacting fuel (tritium) and in the reaction products (neutron and tritium). Category one (radioactivity production):

$T(d,n)\,{}^4He + 17589\ keV$ (1)

$D(d,n)\,{}^3He + 3269\ keV$ (2)

$D(d,p)\,T + 4033\ keV$ (3)

$T(T,2n)\,{}^4He + 11332\ keV$ (4)

Category two (little or no radioactivity production):

${}^3He(d,p)\,{}^4He + 18353\ keV$ (5)

${}^6Li(p,{}^3He)\,{}^4He + 4018\ keV$ (6)

${}^{11}B(p,2\,{}^4He)\,{}^4He + 8681\ keV$ (7)

${}^3He({}^3He,2p)\,{}^4He + 12860\ keV$ (8)

Reaction (5) is not fully aneutronic due to the D-D reactions, but deuterium – helium-3 reaction has the highest known specific fusion power. Positive power output for the ignition and sustainment (plasma gain or amplification factor ~ 10) of a D-^{3}He plasma may be reached at 40-90 keV [13-15]. Reaction (8) has no direct and indirect radioactivity at all.

Section 2 describes the FRC plasma. A reference case is exhibited, and comparison of D-^{3}He tokamak and FRC reactors are discussed in Sec. 3.

2. FRC Fusion Core

Typical pictures of the magnetic flux function, calculated according to Steinhauer analytical equilibrium model (SAE) [16], are shown in Fig. 2. Upper one is relevant to FRC conceptual projects and presents elongated Hill's vortex [17] with elongation $E = l_s / r_s = 5-15$. Racetrack is shown below with $E = 3-5$ that is characteristic for experimental parameters. Parameters used for the calculation are averaged for the experiments and reactors.

Note that paper [16] has type errors. The right expression for the shape index is [18]:

$$N \equiv b^2 / aR_s = \frac{4\varepsilon E_1 + 3\alpha\lambda^5 E_2}{\varepsilon^2\left[-\varepsilon E_1 + \varepsilon\lambda(2+\lambda^2)E_2\right]},$$

where $\lambda = 1/\left[1+(\alpha/\varepsilon)^2\right]^{1/2}$.

It is difficult to find exact Grad-Shafranov solutions to match the cylindrical flux excluding boundary for an FRC. It is especially difficult to find solutions for an elongated FRC or one with more racetrack like separatrix than the elliptical type profile. Models [17,19] have elongated configuration (ellipsoid) and do not have an analytic external solution. But experiments have elongated shape like racetrack. SAE satisfies both experiments and reactor regimes and is a more general equilibrium with external and internal solutions.

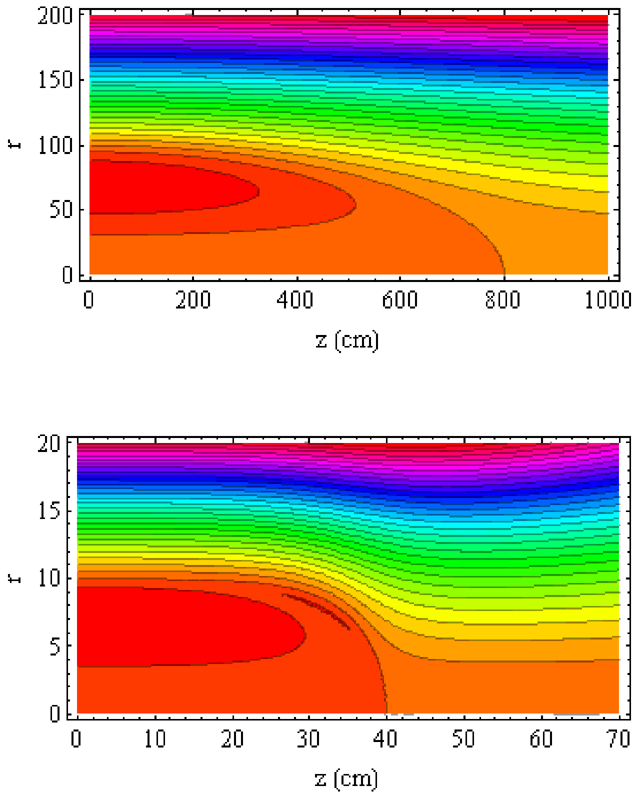

Fig.2 Contour plot of the flux magnetic function for a prolate field reversed configuration: 1) elongated Hill's vortex, B_0 = 10 T, l_s = 8 m, r_s = 1 m, and 2) racetrack equilibrium, B_0 = 1 T, l_s = 0,4 m, r_s = 0,1 m.

The physics and models used in the present analysis are described in details in papers [1,2]. So, only improved Bauman formulas [20] for the total bremsstrahlung losses (power in MW/m^3) including radiation on both ions and electrons are presented here:

$$P_{ei} = 1.7\cdot 10^{-35} n_e^2 y^{1/2} Z_{eff}\left[Log(2y+0.5) + 0.928\right] + \exp(-2y), \qquad (10)$$

$$P_{ee} = 2.57\cdot 10^{-35} n_e^2 y^{3/2}\left[1+1.17y+0.28y^2-0.6y^3\right], \qquad 11)$$

where n_e is the electron density, Z_{eff} is the effective charge, $y = 10^3 T_e e/(m_e c^2)$, T_e is the electron temperature in keV, e is the electron charge, m_e is the electron mass, and c is the speed of light.

The main radiation loss channel in hot FRC D-^{3}He plasmas is bremsstrahlung, which gets over 20% of the total fusion power. Bremsstrahlung loss is soft x-ray radiation that cannot be converted directly to electricity as can charged power particle or, possibly, synchrotron radiation. The correct bremsstrahlung radiation power is shown in Fig. 3. Comparison made with [21-23].

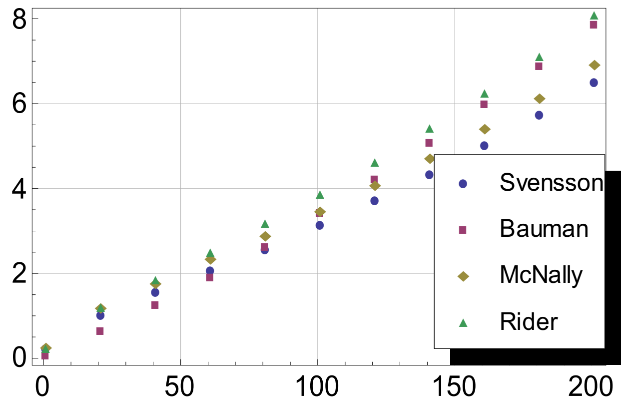

Fig.3 Bremsstrahlung power per unit volume plotted versus electron temperature. Calculations made for the electron density n_e=5 10^{20} m^{-3} and the impurity coefficient Z_{imp}=1.75. The Bauman fit described in the text is shown as boxes.

Bremsstrahlung may be estimated with good accuracy by these formulas. Bauman fit is more precise for the temperature range 10-100 keV that is crucial for aneutronic fusion.

The impact on reactor application is significant. Difference in bremsstrahlung losses just 3% essentially changes power balance and leads to decreasing of fusion amplification factor. So, correct calculation of bremsstrahlung is very important, especially for low radioactive fuel.

The ratio S^*/k has been used to delineate FRC stability regimes, where $k = L_s/r_s$ is the plasma elongation, and S^* is defined by

$$S^* = r_s\,\omega_{pi}/c \approx 0.3\, r_s/\rho_i, \qquad (12)$$

where L_s is the separatrix length, ω_{pi} is the ion plasma frequency, ρ_i is the ion gyroradius, and c/ω_{pi} is comparable to the ion gyroradius for $\beta \approx 1$.

Although definitive limits on S^*/k or S^*/E have not yet been established, the condition of gross stability for present experiments leads to the condition $S^*/E \le 3.5$. Anticipating improvement and because the large fusion-product gyroradii will contribute to FLR stabilization, $S^*/k \le 3.5$ is used for the reactor study, for this paper's reference case. Figure 4 shows FRC operating regimes [24] for some experimental devices and design projects.

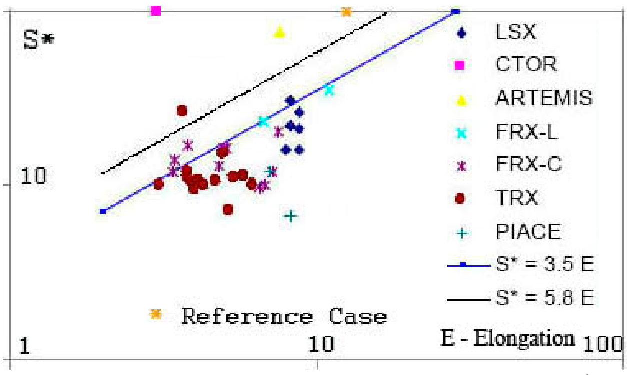

Fig.4 Operating regimes for experimental FRCs and D-^{3}He FRC conceptual power plants.

3. Reactor Study

Table 1 Comparison of the main parameters for D-^{3}He tokamak (T) and FRC power plants (reactor study).

Parameter	*Apollo* (T)	*ARIES-III* (T)	*Artemis* (FRC)	*D-^{3}He FRC (RC)*
Electrical power	1000 MW	1000 MW	1000 MW	1000 MW
Fusion power	2144 MW	2682 MW	1610 MW	1962 MW
Bremsstrahlung	652 MW	Radiation fraction	Total radiation	776 MW
Synchrotron radiation power	1027 MW	0.72	357 MW	8.7 MW
Transport power	456 MW		1181 MW	1188 MW
Neutron power	147 MW	110 MW	77 MW	51.7 MW
Injected (current drive) power	(138 MW)	(172 MW)	5 MW	62.6 MW
Net efficiency	0.43	Recirc. power 0.24	0.36-0.62	0.49
Neutron wall load	5.7 MW/m^2	Aver. 0.08 MW/m^2	0.27 MW/m^2	0.15 MW/m^2
^{3}He to D density ratio	0.63	~ 1	0.5	1
Plasma major(separatrix) radius	7.89 m	7.5 m	1.12 m	1.23 m
Minor radius (separatrix length)	2.5 m	2.5 m	17 m	30.75 m
Ion temperature	57 keV	55 keV	87.5 keV	68.5 keV
Electron temperature	51 keV	53 keV	87.5 keV	68.5 keV
Electron density	1.9 x 10^{20} m^{-3}	3.3 x 10^{20} m^{-3}	6.6 x 10^{20} m^{-3}	5.4 x 10^{20} m^{-3}
Ion density	1.3 x 10^{20} m^{-3}	2.1 x 10^{20} m^{-3}		3.46 x 10^{20} m^{-3}
Plasma current (I/k)	53 MA	30 MA	160 (21) MA	298.8 (24) MA
TF on axis (external B-field)	10.9 (19.3) T	7.6 T	(6.7) T	(6.38) T
Averaged beta	6.7 %	Toroidal 24 %	90 %	74.8 %
Energy confinement time	16 s	11.8 s, $\tau_p/\tau_E = 2$	2.1 s	1.44 s

Reference case (RC) is presented in Table I. Four main D-^{3}He conceptual designs are shown: Apollo [25] and ARIES-III [26] are D-^{3}He fueled tokamaks, Artemis [27] together with the last one proposed by the author are D-^{3}He FRC reactors.

We see in Table I substantial advantages of D-^{3}He FRC power reactors: higher charged particle transport power and β, lower injected power and magnetic field. The advantages of D-^{3}He tokamaks: lower temperature and higher energy confinement time.

The reference case possesses a high plasma current, but it is important to recognize that this current stretches axially along the device and has a short poloidal path. For this reason, the current/elongation *I/k* is a better index of the difficulty in creating and maintaining the current. For this design *I/k*=24 MA. The analogous value in, for example, a D-^{3}He spherical tokamak power plant, is I ~70 MA, in that case for fusion power 1400 MW.

The recent Artemis conceptual D-^{3}He FRC power plant design differs from these assumptions by invoking field-reversed theta-pinch FRC formation, translation from the formation chamber to a burn chamber where neutrals beams sustain the plasma, and traveling wave direct conversion of the ~15 MeV D-^{3}He fusion-product protons before they slow down on the background plasma (energy confinement time $\tau_E = 0$).

Because of small neutron wall load the power plant wastes will be have low radiatioactivity. FRC using advanced fuel has the following best parameters: lower neutron wall load ~ 0.2 MW/m^2 and higher fusion power density ~ 15 MW/m^3.

The optimum size of a reactor based on CT has r_s little larger than thickness of the blanket, shield and coil where r_s is the smallest characteristic size. Comparison with a conceptual D-^{3}He tokamak power plant design indicates that a D-^{3}He FRC reactor would be even more attractive.

In addition, a few projects investigated advanced fuel cycles (with D-D and D-^{3}He) and non-electric applications of fusion along with technological means to lessen the likelihood of proliferation [28-33].

I am indebted to John Santarius for his interest and advice in this research.

This work was supported by the Federal Agency for Science and Innovations Rosnauka (Grant of the President of the Russian Federation № MK-676.2008.8) and Russian Foundation for Basic Research (RFBR Grants № 09-08-00137-a and № 08-08-09244-mob_z).

References

[1] J.F. Santarius *et al.*, Report UWFDM-1129 (2000). See http://fti.neep.wisc.edu/pdf/fdm1129.pdf.

[2] S.V. Ryzhkov *et al.*, Fusion Science and Technology **43** (1T), 304 (2003).

[3] M. Tuszewski, Nucl. Fusion **28**, № 11, 2033 (1988).

[4] R.Kh. Kurtmullaev *et al.*, in book *Results of science and technique. Plasma Physics* Ser. **7**, edited by V.D. Shafranov (VINITI, Moscow, in Russian), 80 (1985).

[5] A.L. Hoffman, FRCs *Course AA559*, University of Washington (2007). hoffman@aa.washington.edu.

[6] A.L. Hoffman *et al.*, *22nd IAEA Fusion Energy Conference* (Geneva, 2008). See http://www.fec2008.ch/preprints/ic_p4-1.pdf.

[7] I. Jones, Phys. Plasmas **6**, № 5, 1950 (1999).

[8] A.L. Hoffman *et al.*, Fusion Science and Technology **41**, 92 (2002).

[9] H.-S. Bosch, and G.M. Hale, Nuclear Fusion **32**, № 4, 611 (1992); Nuclear Fusion **33**, №12, 1919 (1993).

[10] W.M. Nevins, and R. Swain, Nuclear Fusion **40**, № 4, 865 (2000).

[11] R. Feldbacher, *Nuclear reaction cross sections and reactivity parameter library and files* (Vienna: IAEA, 1987).

[12] FENDL, http://www-nds.iaea.org/fendl/fen-fusion.htm.

[13] G.H. Miley, Nuclear Instruments and Methods **207**, 111 (1983).

[14] W. Kernbichler, Fusion Technol. **21**, 2297 (1992).

[15] S.V. Ryzhkov *et al*., Fusion Technol. **39**, 410 (2001).

[16] L.C. Steinhauer, Phys. Fluids B **2**, № 12, 3081 (1990).

[17] M.J. Hill, Philos. Trans. R. Soc. Ser. A., Pt.**1**, C/XXXV, 213 (1894).

[18] Loren Steinhauer, private communication.

[19] L.S. Solov'ev, in *Reviews of Plasma Physics* **6**, edited by M. Leontovich (Consultants Bureau, New York), 239 (1976).

[20] A.Yu. Chirkov *et al.*, Fusion Science and Technology **39** (1T), 402 (2001); V.I. Khvesyuk *et al.*, in *Proc. of II Russian National Conf. on Heat Exchange* **6** (MPEI, Moscow, in Russian), 382 (1998).

[21] R. Svensson, Astrophys. J. **258**, 335 (1982).

[22] J.R. McNally, Nuclear Technology/Fusion **2**, 9 (1982).

[23] T.H. Rider, Phys. Plasmas **2**, № 6, 1853 (1995).

[24] R.E. Siemon *et al.*, *ITC-12* (Toki, 2001).

[25] G.L. Kulcinski *et al.*, Fusion Technol. **21**, 2292 (1992).

[26] F. Najmabadi *et al.*, Report UCLA-PPG-1384. 1994 http://aries.ucsd.edu/LIB/REPORT/ARIES-3/final.shtml.

[27] H. Momota *et al.*, Fusion Technol. **21**, 2307 (1992).

[28] B. Coppi *et al.*, Fusion Technol., **25**, 353 (1994).

[29] M.V. Krivosheev, and V.N. Litunovsky, Fusion Technol. **27** (1T), 337 (1995).

[30] N. Rostoker *et al.*, *Science* **278**, 1419 (1997).

[31] M.J. Schaffer *et al.*, *US-Japan Workshop on Physics of Compact Toroid Plasmas* (Seattle, 2002). See http://www.aa.washington.edu/AERP/RPPL/us-japan-feb-2002/schaffer.pdf.

[32] S.A. Cohen *et al.*, Phys Plasmas **14**, 072508 (2007).

[33] J.F. Santarius, G.L. Kulcinski, L.A. El-Guebaly, Fusion Science and Technol. **44**, 289 (2003).